Density Functional Study on the Regioselectivity of Styrene Polymerization with an *ansa*-Metallocene Catalyst

Sung Hoon Yang, June Huh, and Won Ho Jo*

Hyperstructured Organic Materials Research Center and School of Materials Science and Engineering, Seoul National University, Seoul 151-742, Korea

Received September 20, 2005

The mechanism of regioselectivity of styrene polymerization with a Cp-based *ansa*-matallocene catalyst (Cp = η^5-C_5H_5) was investigated using density functional theory (DFT). The metallocene catalyst studied in this work, $(CH_3)_2SiCp_2Ti(CH_3)_2$, is known to produce polystyrene via the secondary insertion of styrene. A cationic species, $SiH_2Cp_2Ti^+-CH_3$, is used as an activated form of the catalyst for modeling the initiation of styrene polymerization. The results show that primary insertion is more favorable than secondary insertion in the initiation of styrene polymerization, and the most stable product obtained from primary insertion blocks an additional primary insertion of styrene monomer. For propagation of styrene polymerization, secondary insertion is more favorable than primary insertion. If primary insertion occurs during the propagation, the most stable product of the primary insertion blocks again the additional primary insertion of styrene and thus enhances the secondary insertion. The main driving force blocking the primary insertion is the repulsive interaction between two phenyl rings of the preinserted styrene and the next approaching styrene.

I. Introduction

Since the first preparation of syndiotactic polystyrene using metallocene catalysts in 1985,[1] the metallocene-based polymerization of styrene for syndiotactic polystyrene has attracted much interest from industry during the last two decades. Many experimental studies have been performed to elucidate the mechanism of the metallocene-based polymerization of syndiotactic polystyrene.[2] These studies have provided us with very informative structural descriptions for the relationship between the ligand structure of the metallocene catalyst and the tacticity of produced polystyrene.

Nevertheless, there have still been a number of uncertain features in the mechanism of metallocene-based styrene polymerization, which is largely due to the limitation of experimental assessment in investigating the mechanism of styrene insertion into the active site of the metallocene catalyst. As a complementary tool for experimental methods, theoretical calculations based on quantum mechanics have been employed to investigate the mechanism of styrene insertion on a molecular level.[3−5] Theoretical studies on styrene polymerization with metallocene catalyst have given us an insight into the mechanism of styrene insertion, including the structure of the transition state, the activation energy for styrene insertion, and the origin of stereoselectivity of styrene polymerization. As an example, we have recently investigated the mechanism of stereoselectivity of styrene polymerization with an *ansa*-metallocene catalyst using density functional theory (DFT).[3] The metallocene catalyst investigated in the study, $(H_3C)_2SiCp_2Ti(CH_3)_2$ (Cp = η^5-C_5H_4), is experimentally known to produce a highly syndiotactic polystyrene,[6] which is opposed to expectations in the sense that the symmetry of the metallocene ligand would result in an atactic form of the product polymer. The origin of this unusual feature of the *ansa*-metallocene catalyst is suggested to come from the repulsive interaction between the phenyl rings of the preinserted styrene and the next approaching styrene monomer.

Theoretical studies, however, have been rarely carried out on styrene polymerization, whereas olefin polymerization has been extensively studied with theoretical calculations.[7−32]

* To whom correspondence should be addressed. E-mail: whjpoly@plaza.snu.ac.kr. Tel: +82-2-880-7192. Fax: +82-2-885-1748.

(1) Ishihara, N.; Seimiya, T.; Kuramono, M.; Uoi, M. *Polym. Prepr. Jpn.* **1986**, *35*, 240.
(2) Schellenberg, J.; Tomotsu, N. *Prog. Polym. Sci.* **2002**, *27*, 1925 and references reported therein.
(3) Yang, S. H.; Huh, J.; Yang, J. S.; Jo, W. H. *Macromolecules* **2004**, *37*, 5741.
(4) Minieri, G.; Corradini, P.; Zambelli, A.; Guerra, G.; Cavallo, L. *Macromolecules* **2001**, *34*, 2459.
(5) Minieri, G.; Corradini, P.; Guerra, G.; Zambelli, A.; Cavallo, L. *Macromolecules* **2001**, *34*, 5379.
(6) Tomotsu, N.; Ishihara, N.; Newman, T. H.; Malanga, M. T. *J. Mol. Catal. A* **1998**, *128*, 167.
(7) Novaro, O.; Blaisten-Barojas, E.; Clementi, E.; Giunchi, G.; Ruiz-Vizcaya, M. E. *J. Chem. Phys.* **1978**, *68*, 2337.
(8) Fuijimoto, H.; Yamasaki, T.; Mizutani, H.; Koga, N. *J. Am. Chem. Soc.***1985**, *107*, 6157.
(9) Kawamura-Kuribayashi, H.; Koga, N.; Morakuma, K. *J. Am. Chem. Soc.* **1992**, *114*, 2359.
(10) Kawamura-Kuribayashi, H.; Koga, N.; Morokuma, K. *J. Am. Chem. Soc.* **1992**, *114*, 8687.
(11) Koga, N.; Yoshida, T.; Morokuma, K. *Organometallics* **1993**, *12*, 2777.
(12) Siegbahn, P. E. M. *Chem. Phys. Lett.* **1993**, *205*, 290.
(13) Weiss, H.; Ehrig, M.; Ahlrichs, R. *J. Am. Chem. Soc.* **1994**, *116*, 4919.
(14) Bierwagen, E. P.; Bercaw, J. E.; Goddard, W. A., III. *J. Am. Chem. Soc.* **1994**, *116*, 1481.
(15) Doremaele, G. H. J.; Meier, R. J.; Iarlori, S.; Buda, F. *J. Mol. Struct.* (*THEOCHEM*) **1996**, *363*, 269.
(16) Linnolahti, M.; Pakkanen, T. A. *Macromolecules* **2000**, *33*, 9205 and references reported therein.
(17) Lanza, G.; Fragala, I. L.; Marks, T. J. *Organometallics* **2001**, *20*, 4006.
(18) Amstrong, D. R.; Pekins, P. G.; Stewart, J. J. P. *J. Chem. Soc., Dalton Trans.* **1972**, 9172.
(19) Cassoux, P.; Crasnifer, F.; Labarre, J.-F. *J. Organomet. Chem.* **1979**, *165*, 303.
(20) McKinney, R. J. *J. Chem. Soc., Chem. Commun.* **1980**, 490.
(21) Balazs, A. C.; Johnson, K. H. *J. Chem. Phys.* **1982**, *77*, 3148.
(22) Shiga, A.; Kawamura, H.; Ebara, T.; Sasaki, T. *J. Organomet. Chem.* **1989**, *266*, 95.

10.1021/om050812+ CCC: $33.50
Publication on Web 02/04/2006

Scheme 1. Two Modes of Regiochemical Insertions of Styrene into Metallocene Catalytic Active Species[a]

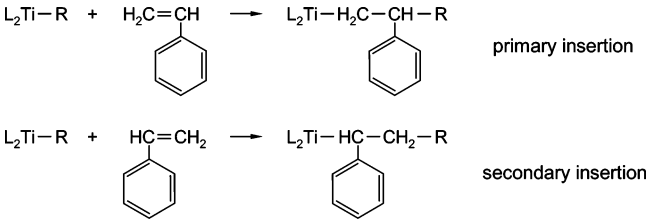

[a] Here, L and R represent the ligand of the catalyst and growing chain, respectively.

Moreover, the theoretical studies on the styrene polymerization have been focused only on the stereoselectivity rather than the regioselectivity of styrene insertion. The regioselectivity of metallocene-based styrene polymerization is referred to as the preference of formation of one chemical bond (e.g., secondary insertion in Scheme 1) over that of the other possible chemical bond (e.g., primary insertion in Scheme 1). The preference of one chemical bonding over others in the styrene insertion highly affects the structure of polystyrene, and therefore, the regioselectivity of metallocene-based styrene polymerization is also as crucially important as the stereoselectivity. However, the origin of the regioselectivity has not been fully understood. For example, the reason styrene polymerization with a metallocene catalyst proceeds via secondary insertion, which is observed from experiments, has still not been unraveled. Indeed, it is contrary to the case of olefin polymerization, where primary insertion is more favorable than secondary insertion. Therefore, it is very important to elucidate the mechanism of regioselectivity of styrene insertion.

In this paper, the regioselectivity of styrene polymerization with an *ansa*-metallocene catalyst has been studied using density functional theory. We have investigated the mechanism of successive insertion of styrene monomers into the acive species of the *ansa*-metallocene catalyst by assuming that the insertion follows the sequence shown in Scheme 2, where possible reaction pathways for the successive insertion of styrene monomers into the active catalyst are illustrated. For insertion of the first styrene monomer, there are two reaction pathways: primary (P) and secondary (S) insertions. After the first styrene insertion, the second insertion of a styrene monomer into each product of the first insertion has also two insertion pathways: i.e., the primary and secondary insertions. Therefore, there are four kinds of regiochemical insertions: primary insertion after primary insertion (PP), secondary insertion after secondary insertion (SS), secondary insertion after primary insertion (PS), and primary insertion after secondary insertion (SP). For the PP or SS insertion, the resulting product forms an isotactic (PPi or SSi) or syndiotactic (PPs or SSs) diad, while for the PS or SP insertion, the resulting product forms a syn (PSs or SPs) or anti (PSa or SPa) diad (Scheme 2). The nomenclature of syn and anti represents the relative position of two styrene phenyl rings with respect to the plane of the chain backbone, when the chain backbone is represented by commonly used zigzag drawings. More specifically, the two phenyl rings of the diad formed by PSs or SPs insertion are toward the same side (syn side) of the chain backbone plane, while those formed by PSa or SPa insertion are toward the opposite side (anti side) of the plane (Scheme 2).

The paper is organized as follows. After a detailed description of the computational methods in the next section, the mechanism of regioselectivity for the initiation of styrene polymerization is discussed in section III. In section IV, we discuss the mechanism of the regioselectivity for propagation of styrene polymerization, and we summarize our main results in section V.

II. Computational Details

The fundamentals of the computational methods are similar to those in our previous works.[3,33,34] All calculations were performed using the DMol[3] program (Accelrys Inc.) based on DFT.[35] Electronic configurations of molecular systems were described by restricted double-numerical basis sets with polarization functions for all atoms, except for hydrogen. The $1s^2 2s^2 2p^6$ configuration on titanium was assigned to the core and treated by the frozen-core approximation. A geometry optimization was carried out using the Broydan−Fletcher−Goldfarb−Shanno[36−38] (BFGS) energy minimization algorithm for each molecule. The general gradient approximation (GGA) correction was applied to the energy calculations with the exchange functional of Becke (B88)[39] and the correlation functional of Perdew and Wang (PW91)[40,41] after the energy was first calculated at the local density approximation (LDA) level.

The cationic methyltitanocene $H_2SiCp_2Ti^+-CH_3$, which is a model of active catalytic species employed successfully in our previous study[3] for investigating the stereoselectivity of styrene insertion, is also used for investigating the regioselectivity of styrene insertion in this study. $H_2SiCp_2Ti^+-CH_3$ is a simplified form of the activated catalytic species of $(CH_3)_2SiCp_2Ti(CH_3)_2$, and the simplification of $(CH_3)_2Si$ by H_2Si in the model catalyst is assumed to have a negligible effect on the reaction mechanism, although the electronic charge density on the Si atom might be slightly changed. The insertion of a styrene monomer was performed by a stepwise decrease in the reaction coordinate, followed by optimization of geometry with respect to all other degrees of freedom at each step. The reaction coordinate is defined as the distance between the C_α atom (i.e., the carbon which is directly attached to the titanium) and the C_1 atom (i.e., the vinyl carbon of the styrene monomer on which the phenyl group is attached) for the secondary insertion and the distance between the C_α atom and the C_2 atom (i.e., the other vinyl carbon of the styrene monomer) for the primary insertion. A decrease in the reaction coordinate corresponds to an approach of a styrene monomer toward the reactive site of the catalyst. By this stepwise insertion process described above, the reaction undergoes three distinctive states: π-complex, transition

(23) Prosenc, M.-H.; Janiak, C.; Brintzinger, H.-H. *Organometallics* **1992**, *11*, 4036.
(24) Coussens, B. B.; Buda, F.; Oevering, H.; Meier, R. J. *Organometallics* **1998**, *17*, 795.
(25) Woo, T. K.; Fan, L.; Ziegler, T. *Organometallics* **1994**, *13*, 2252.
(26) Fan, L.; Harrison, D.; Deng, L.; Woo, T. K.; Swerhone, D.; Ziegler, T. *Can. J. Chem.* **1995**, *73*, 989.
(27) Lohrenz, J. C. W.; Woo, T. K.; Fan, L.; Ziegler, T. *J. Organomet. Chem.* **1995**, *497*, 91.
(28) Woo, T. K.; Margl, P. M.; Lohrenz, J. C. W.; Blöchl, P. E.; Ziegler, T. *J. Am. Chem. Soc.* **1996**, *118*, 13021.
(29) Margl, P.; Deng, L.; Ziegler, T. *J. Am. Chem. Soc.* **1999**, *121*, 154.
(30) Lohrenz, J. C. W.; Bühl, M.; Weber, M.; Thiel, W. *J. Organomet. Chem.* **1999**, *592*, 11.
(31) Petitjean, L.; Pattou, D.; Ruiz-Lopez, M. −F. *J. Mol. Struct.* (*THEOCHEM*) **2001**, *541*, 227.
(32) Vanka, K.; Chan, M. S. W.; Pye, C. C.; Ziegler, T. *Macromol. Symp.* **2001**, *173*, 163.
(33) Yang, S. H.; Jo, W. H.; Noh, S. K. *J. Chem. Phys.* **2003**, *119*, 1824.
(34) Yang, S. H.; Huh, J.; Jo, W. H. *Macromolecules* **2005**, *38*, 1402.
(35) Delly, B. *J. Chem. Phys.* **1991**, *94*, 7245.
(36) Press: W. H.; Flannery, B. P.; Teukolsky, S. A.; Vetterling, W. T. *Numerical Recipes, the Art of Scientific Computing*; Cambridge University Press: New York, 1986.
(37) Pulay, P. *J. Comput. Chem.* **1982**, *3*, 556.
(38) Csaszar, P.; Pulay, P. *J. Mol. Struct.* **1984**, *114*, 31.
(39) Becke, A. D. *Phys. Rev. A* **1988**, *38*, 3098.
(40) Perdew, J. P.; Wang, Y. *Phys. Rev. B* **1992**, *45*, 13244.
(41) Perdew, J. P.; Chevary, J. A.; Vosko, S. H.; Jackson, K. A.; Pederson, M. R.; Singh, D. J.; Fiolhais, C. *Phys. Rev. B* **1992**, *46*, 6671.

Scheme 2. All Possible Reaction Pathways for the Styrene Monomer Insertion in View of Regiochemistry for Styrene Monomer Insertion

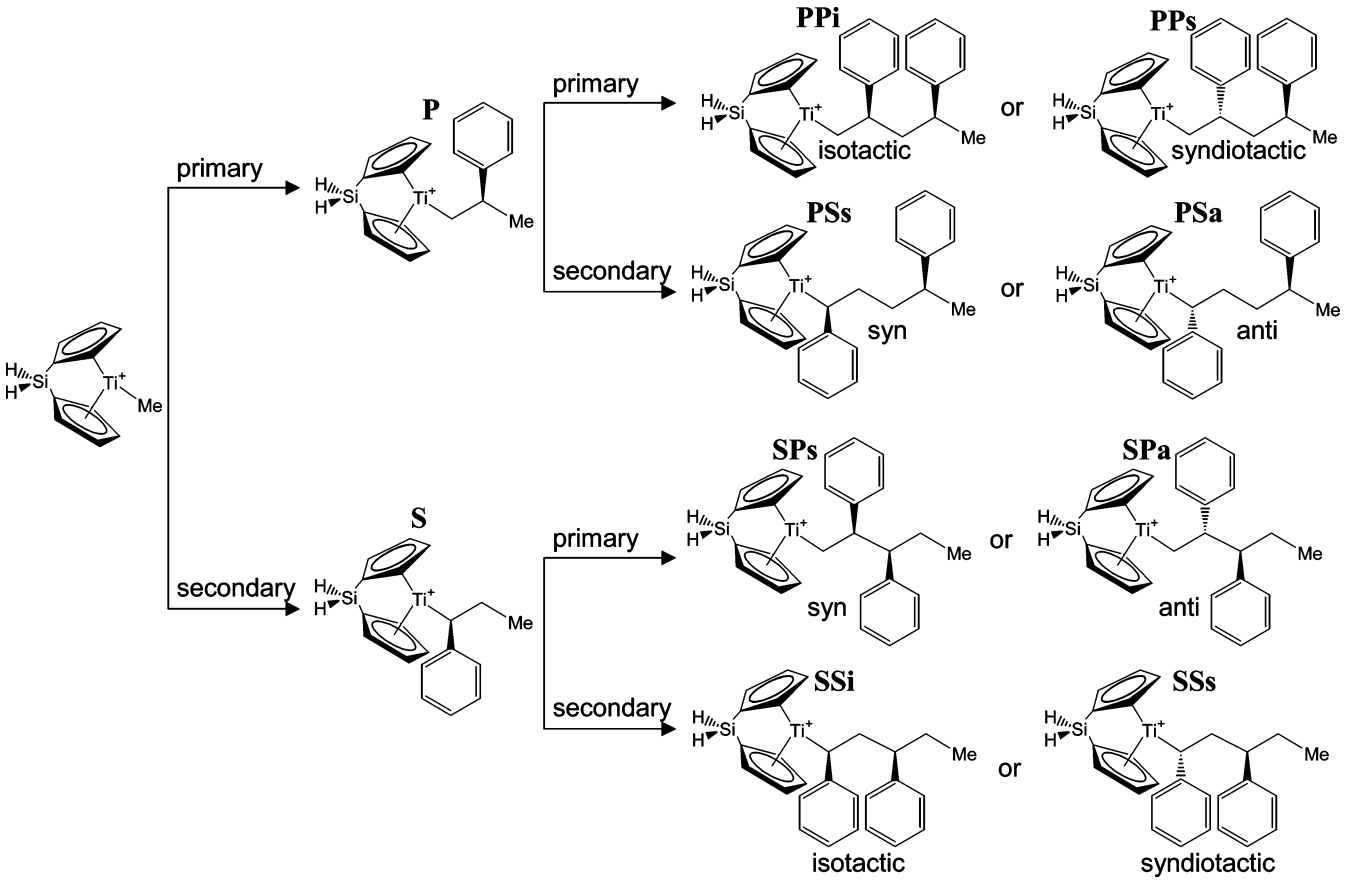

state, and product. The π-complex is a local minimum on the energy profile during monomer insertion, the transition state is a maximum point on the energy profile in the reaction coordinate between complex and product, and the product is the point of minimum energy. This procedure was applied to all of the monomer insertion processes.

III. Regioselectivity of Initiation

Primary insertion of the first styrene monomer into the catalytic site of the cationic methyltitanocene, i.e., H_2SiCp_2-Ti^+-CH_3, was performed. The energy profile of the first styrene insertion with the structure at each of the stationary points is shown in Figure 1. The energy of each structure relative to the sum of energies of the isolated free reactants, i.e., the cationic methyltitanocene and styrene monomer, is denoted at each energy level. To compare the energetics of primary insertion with that of secondary insertion during the first styrene insertion, we also denoted the energies for secondary insertion at the corresponding energy level in parentheses, which are taken from our previous study.[3] The overall behavior of the energy profile for primary insertion is similar to that for secondary insertion: (i) the π-complex is formed through an exothermic process (-18.61 kcal/mol for primary insertion; -19.42 kcal/mol for secondary insertion), (ii) an energy barrier ($\Delta E = 7.45$ kcal/mol for primary insertion; $\Delta E = 9.30$ kcal/mol for secondary insertion) should be overcome for progressing to the product, and (iii) the product is energetically stabilized (-21.91 kcal/mol for primary insertion; -24.16 kcal/mol for secondary insertion) by γ-agostic interactions.

However, when we consider the fact that secondary insertion is experimentally known to be a more favorable process than primary insertion in styrene polymerization with the *ansa*-metallocene catalyst,[6] the result shown in Figure 1 is not understandable, because the activation energy for primary insertion (7.45 kcal/mol) is lower than that for secondary insertion (9.30 kcal/mol). These unexpected energetics have been also reported in previous theoretical studies by Muñoz-Escalona and co-workers,[42,43] although the catalyst in their studies is different from that in our study and they focused on the mechanism of ethylene−styrene copolymerization. The result of their study for the first styrene insertion into their active catalyst shows that the activation energy for secondary insertion is higher than that for primary insertion, which is obviously inconsistent with the fact that the catalyst of their study is experimentally observed to favor secondary insertion of the styrene monomer over primary insertion during the copolymerization. To rationalize their result, they argued that the regioselectivity of the styrene insertion depends on the stability of the product conformer: the most stable conformer of the product formed via the primary insertion is an inactive species for further polymerization, because the phenyl ring of the last inserted styrene monomer blocks the active site of the catalytic species due to the presence of a strong interaction between the phenyl ring and the metal center of the catalyst. We call the interaction between the phenyl ring of the last styrene unit in the growing chain and the metal center of the catalyst a "ϕ (phenyl)−agostic interaction" in this study.

(42) Muñoz-Escalona, A.; Cruz, V.; Mena, N.; Martínez, S.; Martinez-Salazar, J. *Polymer* **2002**, *43*, 7017.

(43) Martínez, S.; Cruz, V.; Muñoz-Escalona, A.; Martinez-Salazar, J. *Polymer* **2003**, *44*, 295.

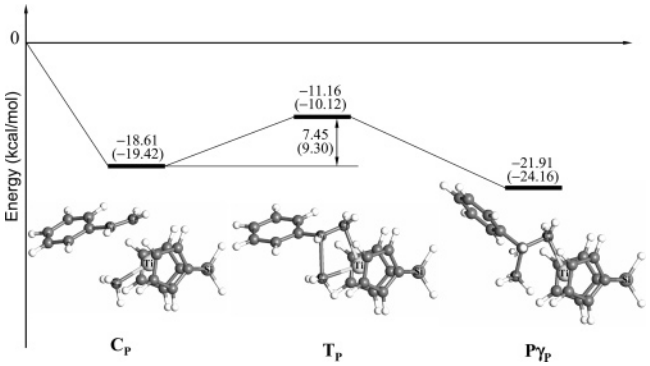

Figure 1. Energy profile and structures of the complex (**C_P**), transition state (**T_P**), and product (**$P\gamma_P$**) during the initiation of styrene polymerization via the primary insertion of styrene monomer. Energies are relative to the energies of isolated free reactants. The energies for secondary insertion at the corresponding energy level are given in parentheses.

To clarify the nature of the interaction between the Ti atom and the phenyl group, we calculated the charges of the Ti atom and the C atoms of the cyclopentadienyl (Cp) ligand and the phenyl ring by Hirshfeld population analysis.[44,45] The Ti charge is 0.376, and the charges of the C atoms (C_{Ph}) of the phenyl ring are −0.055, −0.014, −0.023, −0.023, −0.001, and 0.038. Considering that the charges of the C atoms of the Cp ligand range from −0.090 to −0.023 (see the Supporting Information), where the interaction is known to be coordinative, the interaction between Ti and the phenyl ring may be also referred to as a coordinative interaction. Second, the distance between the Ti and a C_{Ph} atom of the phenyl ring, 2.517 Å, is as short as the average distance between Ti and the C atoms of the Cp ligand, 2.412 Å. This indicates that the interaction between the Ti atom and the phenyl carbon is as strong as the coordinative interaction between the Ti atom and the Cp ligand. Therefore, the strong interaction between the Ti atom and the phenyl ring may be referred to as a coordinative interaction rather than an electrostatic interaction.

Indeed, the ϕ-agostic interaction is stronger than the other agostic interactions such as γ-agostic and β-agostic interactions, which is obvious from the result that the conformer showing an ϕ-agostic interaction, i.e., the ϕ-agostic product (**$P\phi_P$** in Figure 2, −30.24 kcal/mol), is more stable than the γ-agostic (**$P\gamma_P$** in Figure 1, −21.91 kcal/mol) and the β-agostic products (**$P\beta_P$** in Figure 2, −28.98 kcal/mol). Moreover, the conformers formed by a chain back-skip (**$P\beta'_P$** and **$P\phi'_P$** from **$P\beta_P$** and **$P\phi_P$**, respectively), i.e., an inversion of the Ti−C_α bond vector with respect to the Cen−Ti−Cen plane, where Cen represents the center of the cyclopentadienyl ring, are less stable than the ϕ-agostic product, as shown in Figure 2 (**$P\beta'_P$**, −27.68 kcal/mol; **$P\phi'_P$**, −28.84 kcal/mol). These results are very consistent with those of Muñoz-Escalona et al.:[42] i.e., the ϕ-agostic product, which does not allow polymerization of another styrene, is the most stable conformer among the various product conformers.

However, the explanation described above is still unsatisfactory, because there remains a critical problem in the explanation: if the ϕ-agostic product blocks an additional insertion of the styrene monomer, how could the catalyst show high catalytic activity, even though most of the catalytically active species become inactive species by primary insertion, which is kinetically faster than secondary insertion at the initiation stage? To solve this problem, we have calculated the energetics for the

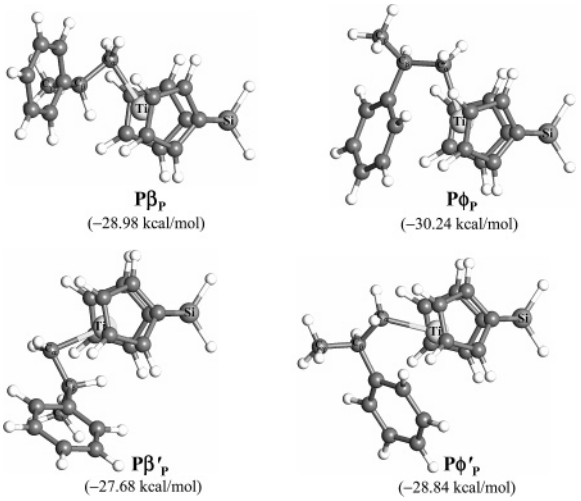

Figure 2. Structures of various product conformers formed by primary insertion: β-agostic product (**$P\beta_P$**), back-skip of the β-agostic product (**$P\beta'_P$**), ϕ-agostic product (**$P\phi_P$**), and back-skip of the ϕ-agostic product (**$P\phi'_P$**).

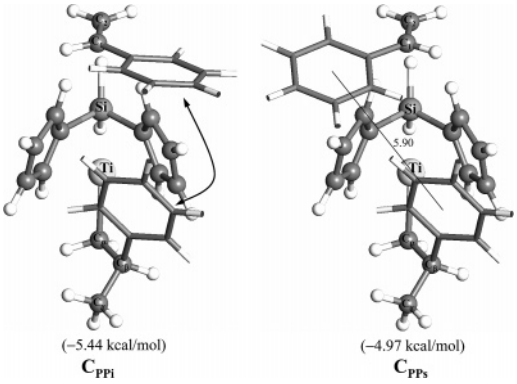

Figure 3. Side views of complexes formed by primary isotactic insertion (**C_{PPi}**) and primary syndiotactic insertion (**C_{PPs}**) into the product of the first primary insertion.

insertion of another styrene monomer into the ϕ-agostic product, **$P\phi_P$**. There are four types of styrene insertion into **$P\phi_P$**: (i) isotactic primary insertion (PPi), (ii) syndiotactic primary insertion (PPs), (iii) syn-side secondary insertion (PSs), and (iv) anti-side secondary insertion (PSa) (see Scheme 2).

First, when the structures of π-complexes for the two primary insertions into $P\phi_P$ (**C_{PPi}** for isotactic and **C_{PPs}** for syndiotactic primary insertions) are shown in Figure 3, it can be seen that the two phenyl rings of the preinserted and the next approaching styrene monomers are located on the same side of the plane defined by Ti, Si, and C_α atoms in **C_{PPi}**, whereas the two phenyl rings are located on opposite sides of the Ti−Si−C_α plane in **C_{PPs}**. Moreover, when the energetics for isotactic primary insertion into **$P\phi_P$** (i.e., PPi insertion) are calculated as a function of the reaction coordinate (distance between C_α and C_1 atoms), they reveal that the structure is converted into an abnormal structure which is impossible of yielding a product of styrene insertion, due to the high repulsive interaction between the two phenyl rings. Therefore, it is concluded that the isotactic primary insertion after the primary insertion of styrene monomer is blocked, due to the high repulsive interaction between the two phenyl rings of the preinserted and the next approaching styrene monomers during polymerization.

In contrast to the isotactic primary insertion, the syndiotactic primary insertion seems not to be blocked, because the activation energy for the syndiotactic primary insertion into **$P\phi_P$** is only

(44) Hirshfeld, F. L. *Theor. Chem. Acta* **1977**, *44*, 129.
(45) Delley, B. *J. Chem. Phys.* **1990**, *92*, 508.

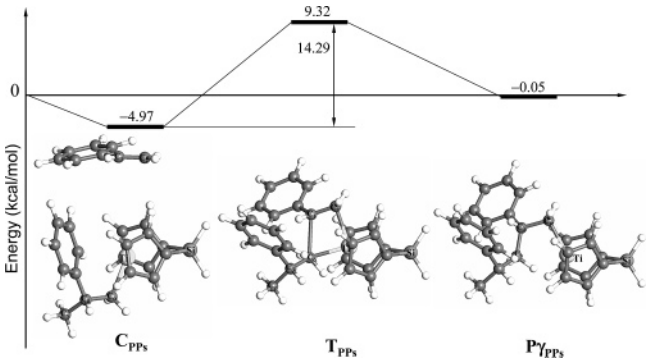

Figure 4. Energy profile and structures of the complex ($\mathbf{C_{PPs}}$), transition state ($\mathbf{T_{PPs}}$), and product ($\mathbf{P\gamma_{PPs}}$) during the primary syndiotactic insertion of styrene monomer after the first primary insertion. Energies are relative to the energies of isolated free reactants.

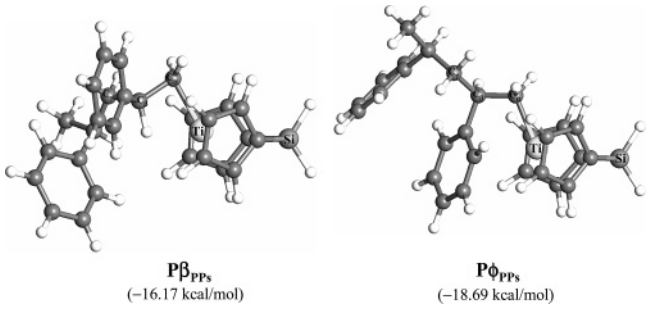

Figure 5. Structures of the β-agostic ($\mathbf{P\beta_{PPs}}$) and the ϕ-agostic ($\mathbf{P\phi_{PPs}}$) products of primary syndiotactic insertion of the second styrene into the product of the first primary insertion.

14.29 kcal/mol (see Figure 4), which corresponds to the typical value of activation energy for styrene insertion in propagation (∼15 kcal/mol). This interesting result suggests that the strong stability of a ϕ-agostic product is not evidence for the inactivation of catalytically active species, and therefore, it cannot rationalize the preference of secondary insertion over the primary insertion during styrene polymerization, although we accept the fact that the ϕ-agostic interaction is stronger than any other agostic interactions.

The relative stability of product conformers obtained from primary insertion is applicable to all insertion pathways: for the first insertion and the second insertion, the ϕ-agostic product ($\mathbf{P\phi_P}$ in Figure 2, −30.24 kcal/mol; $\mathbf{P\phi_{PPs}}$ in Figure 5, −18.69 kcal/mol) is more stable than the γ-agostic ($\mathbf{P\gamma_P}$ in Figure 1, −21.91 kcal/mol; $\mathbf{P\gamma_{PPs}}$ in Figure 4, −0.05 kcal/mol) and the β-agostic products ($\mathbf{P\beta_P}$ in Figure 2, −28.98 kcal/mol; $\mathbf{P\beta_{PPs}}$ in Figure 5, −16.17 kcal/mol). In other words, the ϕ-agostic product is the most stable conformer, i.e., the resting state, for the primary insertion of styrene monomer.

The structures of π-complexes for the secondary insertions into $\mathbf{P\phi_P}$ are shown in Figure 6 ($\mathbf{C_{PSs}}$ for syn-side and $\mathbf{C_{PSa}}$ for anti-side secondary insertions). We do not consider the syn-side insertion (PSs) in the following discussion for the secondary insertion of styrene into $\mathbf{P\phi_P}$, because the two phenyl rings in $\mathbf{C_{PSs}}$ are located on the same side of the Ti−Si−C_α plane. The energy profile and the structures of the stationary points during the anti-side secondary insertion into $\mathbf{P\phi_P}$ (PSa) are shown in Figure 7. It is very surprising that the activation energy for the anti-side secondary insertion is considerably lower (6.30 kcal/mol) than that for the syndiotactic primary insertion (14.29 kcal/mol in Figure 4), which means that secondary insertion into $P\phi_P$ is favored considerably over primary insertion. Conclu-

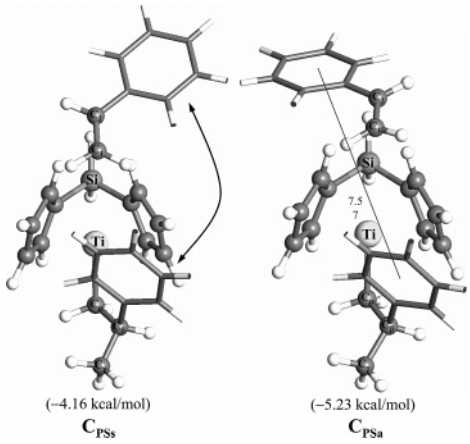

Figure 6. Side views of complexes formed by secondary syn-side insertion ($\mathbf{C_{PSs}}$) and secondary anti-side insertion ($\mathbf{C_{PSa}}$) into the product of the first primary insertion.

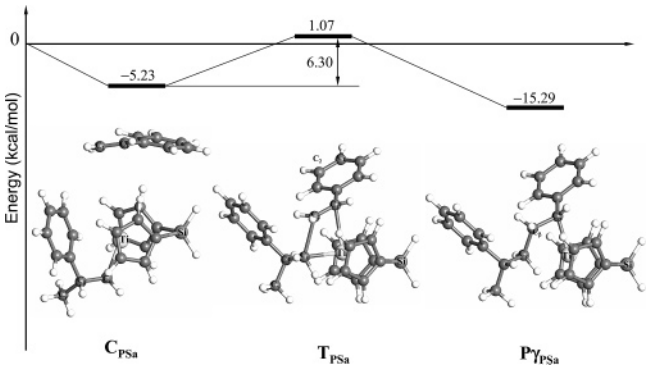

Figure 7. Energy profile and structures of the complex ($\mathbf{C_{PSa}}$), transition state ($\mathbf{T_{PSa}}$), and product ($\mathbf{P\gamma_{PSa}}$) during the secondary anti-side insertion of styrene monomer after the first primary insertion. Energies are relative to the energies of isolated free reactants.

sively, this result suggests that, if primary styrene insertion occurs in the initiation of styrene polymerization, secondary styrene insertion occurs favorably over primary insertion in the next styrene insertion. The reason for the considerably lower activation energy for secondary styrene insertion as compared to that for primary insertion is thought to be the lower repulsive interaction between the two phenyl rings in secondary insertion as compared to that in primary insertion. For instance, the distance between the two phenyl rings in secondary insertion ($\mathbf{C_{PSa}}$ in Figure 6, 7.57 Å) is somewhat longer than that in primary insertion ($\mathbf{C_{PPs}}$ in Figure 3, 5.90 Å), where the distance of the two phenyl rings is defined by the distance between the centers of the phenyl rings.

The γ-agostic product ($\mathbf{P\gamma_{PSa}}$ in Figure 7, −15.29 kcal/mol), which is directly produced via secondary styrene insertion, is transformed into a more stable conformer, the β-agostic product ($\mathbf{P\beta_{PSa}}$ in Figure 8, −23.39 kcal/mol). Finally, the resting structure ($\mathbf{P\beta'_{PSa}}$ in Figure 8, −26.62 kcal/mol) is formed via back-skip from the β-agostic product ($\mathbf{P\beta_{PSa}}$), which is responsible for the successive backside insertions of styrene monomers, resulting in syndiotactic polystyrene, as suggested in our previous study.[3] Conclusively, if primary insertion of styrene monomer occurs in the initiation of styrene polymerization, the next insertion of styrene monomer proceeds via secondary insertion preferably over primary insertion. Therefore, we define the ϕ-agostic product as a product blocking the primary insertion of styrene during styrene polymerization.

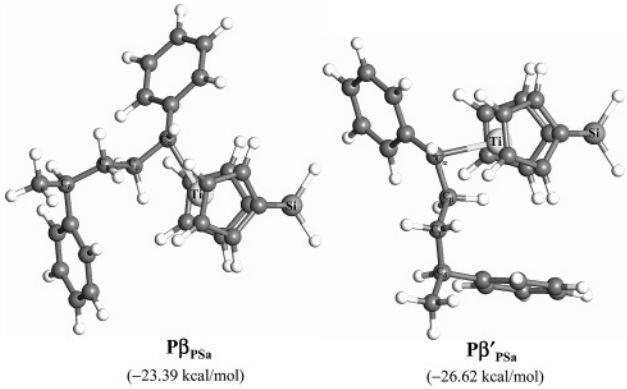

Figure 8. Structures of the β-agostic product ($\mathbf{P}\beta_{\mathbf{PSa}}$) and the back-skip of the β-agostic product ($\mathbf{P}\beta'_{\mathbf{PSa}}$) obtained from the secondary anti-side insertion of the second styrene into the product of the first primary insertion.

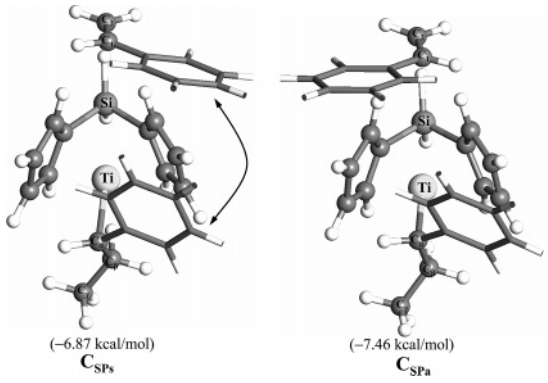

Figure 9. Side views of complexes formed by the primary syn-side insertion ($\mathbf{C}_{\mathbf{SPs}}$) and the primary anti-side insertion ($\mathbf{C}_{\mathbf{SPa}}$) into the product of the first secondary insertion.

IV. Regioselectivity of Propagation

To investigate the regioselectivity during the propagation of styrene polymerization, we have performed calculations for the insertion of styrene monomer into the product of the first secondary styrene insertion: i.e., $H_2SiCp_2Ti^+-CH(C_6H_5)CH_2-CH_3$. The most stable conformation of the product, which is denoted as $\mathbf{P}\beta'_{\mathbf{S}}$ in this study, is used as an active species for the second styrene insertion. The $\mathbf{P}\beta'_{\mathbf{S}}$ is formed by a back-skip from the β-agostic product ($\mathbf{P}\beta_{\mathbf{S}}$), as described in detail in our previous study.[3]

There are four modes in the second styrene insertion into $\mathbf{P}\beta'_{\mathbf{S}}$: (i) syn-side primary insertion (SPs), (ii) anti-side primary insertion (SPa), (iii) isotactic secondary insertion (SSi), and (iv) syndiotactic secondary insertion (SSs) (see Scheme 2). The last two secondary insertions among the four insertion modes, i.e., SSi and SSs, were elaborately investigated in our previous study,[3] where the mechanism for the stereoselectivity of styrene polymerization has been suggested. Here, we report the mechanism for the SPs and SPa insertion modes.

The π-complexes for primary insertions into $\mathbf{P}\beta'_{\mathbf{S}}$, i.e., $\mathbf{C}_{\mathbf{SPs}}$ and $\mathbf{C}_{\mathbf{SPa}}$, are shown in Figure 9. Both $\mathbf{C}_{\mathbf{SPs}}$ and $\mathbf{C}_{\mathbf{SPa}}$ show sterically hindered repulsion between the two phenyl rings of the preinserted and the next approaching styrene monomer. The energetics and structure for the syn-side primary insertion of styrene monomer (SPs) into $\mathbf{P}\beta'_{\mathbf{S}}$ are shown in Figure 10. The energetics indicate that the SPs insertion is almost impossible ($\Delta E = 24.83$ kcal/mol), because the two phenyl rings of the preinserted and the next approaching styrene monomer are located on the same side of the Si−Ti−C_α plane, as depicted

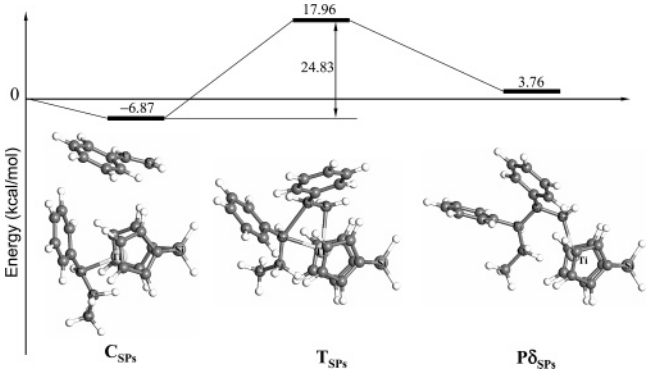

Figure 10. Energy profile and structures of the complex ($\mathbf{C}_{\mathbf{SPs}}$), transition state ($\mathbf{T}_{\mathbf{SPs}}$), and product ($\mathbf{P}\delta_{\mathbf{SPs}}$) during the primary syn-side insertion of styrene monomer after the first secondary insertion. Energies are relative to the energies of isolated free reactants.

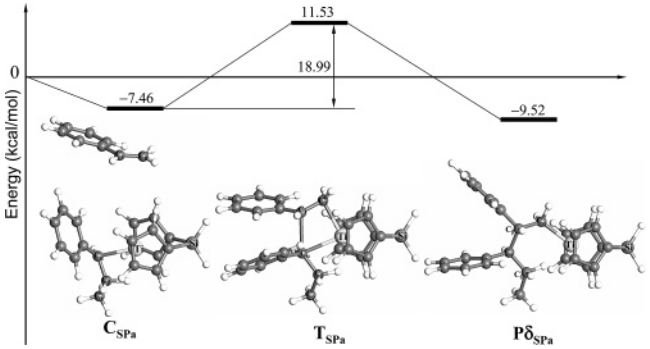

Figure 11. Energy profile and structures of the complex ($\mathbf{C}_{\mathbf{SPa}}$), transition state ($\mathbf{T}_{\mathbf{SPa}}$), and product ($\mathbf{P}\delta_{\mathbf{SPa}}$) during the primary anti-side insertion of styrene monomer after the first secondary insertion. Energies are relative to the energies of isolated free reactants.

in Figure 9 with an arrow. On the other hand, the repulsive interaction between the two phenyl rings for the anti-side primary insertion into $\mathbf{P}\beta'_{\mathbf{S}}$ (SPa) is somewhat lowered ($\Delta E =$ 18.99 kcal/mol in Figure 11), because the two phenyl rings are located on opposite sides of the Si−Ti−C_α plane, as shown in Figure 9. Although the activation energy of SPa insertion (18.99 kcal/mol) is lower than that of SPs insertion (24.83 kcal/mol), the former is still higher than for the secondary insertions, i.e., SSi (18.22 kcal/mol) and SSs (15.20 kcal/mol),[3] which means that secondary styrene insertion is favored over primary styrene insertion into the catalytic species formed by secondary insertion during styrene polymerization. The reason for this higher repulsive interaction between the two phenyl rings in primary insertion as compared to that in secondary insertion into $\mathbf{P}\beta'_{\mathbf{S}}$ is that the phenyl ring of the next approaching styrene conflicts directly with that of the preinserted styrene in the primary insertions, whereas the two phenyl rings are apart farther in the secondary insertion than in the primary insertion. Conclusively, the regioselectivity for propagation of styrene polymerization also originates from the repulsive interaction between the two phenyl rings of the preinserted and the next approaching styrene monomers.

Finally, we optimized β-agostic ($\mathbf{P}\beta_{\mathbf{SPs}}$ and $\mathbf{P}\beta_{\mathbf{SPa}}$) and ϕ-agostic ($\mathbf{P}\phi_{\mathbf{SPs}}$ and $\mathbf{P}\phi_{\mathbf{SPa}}$) product conformers (Figure 12), which are more stable than the δ-agostic product ($\mathbf{P}\delta_{\mathbf{SPs}}$ and $\mathbf{P}\delta_{\mathbf{SPa}}$ in Figure 11). Consistent with the results of all kinds of primary insertion modes (P, PPi, and PPs) considered in this study, the ϕ-agostic product ($\mathbf{P}\phi_{\mathbf{SPs}}$ and $\mathbf{P}\phi_{\mathbf{SPa}}$) is also the most stable conformer. According to the mechanism suggested in section III for the initiation of styrene polymerization, it is strongly expected that the next insertion of styrene monomer

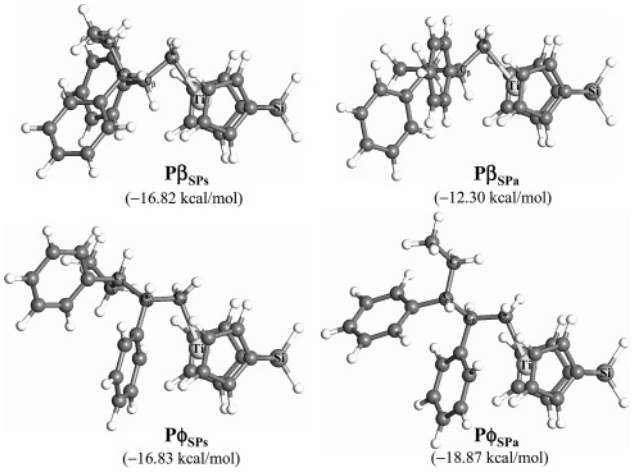

Figure 12. Structures of the β-agostic (**P**$\beta_{\mathbf{SPs}}$ and **P**$\beta_{\mathbf{SPa}}$) and ϕ-agostic products (**P**$\phi_{\mathbf{SPs}}$ and **P**$\phi_{\mathbf{SPs}}$) of primary (syn- and anti-side) insertion of the second styrene into the product of the first secondary insertion.

into **P**$\phi_{\mathbf{SPs}}$ and **P**$\phi_{\mathbf{SPa}}$ proceeds via secondary insertion in preference to primary insertion, because the ϕ-agostic product blocks primary insertion during the styrene polymerization.

V. Summary

A DFT study on the origin of regioselectivity for styrene polymerization with *ansa*-metallocene has been reported. It is found that primary insertion is more favorable than secondary insertion in the initiation of polymerization. However, the product obtained from primary insertion is transformed into the most stable conformer showing a ϕ-agostic structure, which blocks the additional primary insertion of styrene monomer. The main driving force blocking primary insertion is the repulsive interaction between two phenyl rings of the preinserted styrene and the next approaching styrene.

For the propagation of styrene polymerization, secondary insertion is more favorable than primary insertion, which also originates from the repulsive interaction between the two phenyl rings of the preinserted styrene and the next approaching styrene. If primary insertion occurs during propagation, the product of primary insertion is transformed to the most stable ϕ-agostic structure, which blocks the additional primary insertion of styrene while enhancing secondary insertion. As a result, the propagation of styrene polymerization proceeds via secondary insertion of styrene monomers.

One of the limitations in this study is that the counterion interactions were not taken into account during the calculations. The counterion has considerable effects on the energetics of monomer insertion, and the effects are more significant in the initiation of polymerization (the first monomer insertion) than in the propagation, which has been elaborately studied in our previous work[34] on ethylene polymerization with a constrained-geometry catalytic system. However, it is still too time-consuming to include the counterion into the calculation of styrene insertion. Moreover, the counterion interactions are relatively less important in some cases, such as the case where the solvent polarity is high enough to separate the catalytic cation from the counterion, which is the reason the counterion was neglected in this theoretical study. Hence, the mechanism suggested in this study can be modified in a future theoretical study using an advanced model including the counterion interactions and/or solvent polarity.

Acknowledgment. We thank the Korea Science and Engineering Foundation (KOSEF) through the Hyperstructured Organic Materials Research Center (HOMRC).

Supporting Information Available: A figure showing the relationship between the phenyl ring and the metal atom of Pϕ_{P} and a table giving optimized Cartesian coordinates and absolute energies of all stationary points. This material is available free of charge via the Internet at http://pubs.acs.org.

OM050812+